J Mol Neurosci (2015) 57:73–82
DOI 10.1007/s12031-015-0578-6

Scheme of Ischaemia-triggered Agents during Brain Infarct Evolution in a Rat Model of Permanent Focal Ischaemia

Petra Bonova[1] · Viera Danielisova[1] · Miroslava Nemethova[1] · Milina Matiasova[1] · Martin Bona[2] · Miroslav Gottlieb[1]

Received: 17 April 2015 / Accepted: 5 May 2015 / Published online: 14 May 2015

Abstract The impact of therapeutic intervention in stroke depends on its appropriate timing during infarct evolution. We have studied markers of brain tissue damage initiated by permanent occlusion of the middle cerebral artery (MCAO) at three time points during which the infarct spread (1, 3 and 6 h). Based on Evans Blue extravasation and immunohistochemical detection of neurons, we confirmed continuous disruption of blood-brain barrier and loss of neurons in the ischaemic hemisphere that peaked at the sixth hour, especially in the core. Glutamate content started to rise dramatically in the entire hemisphere during the first 3 h; the highest level was determined in the core 6 h after MCAO (141 % increase). Moreover, the enzyme antioxidant defence grew by about 42 % since the first hour in the ipsilateral penumbra. Enzymes of the apoptotic pathway as well as mitochondrial enzyme release were detected since the third hour of MCAO in the ischaemic hemisphere; all achieved their maxima in the penumbra during both time periods (except cytochrome C). In conclusion, the preserved integrity of mitochondrial membrane and incompletely developed process of apoptosis may contribute to the better therapeutic outcome after ischaemic attack; however, a whole brain response should not be omitted.

Keywords Brain · Permanent ischaemia · Core expansion · Ischaemia-triggered agents · Infarct evolution

✉ Petra Bonova
kravcukova@saske.sk

[1] Institute of Neurobiology, Slovak Academy of Sciences, Košice, Slovakia

[2] Department of Anatomy, Faculty of Medicine, Pavol Jozef Safarik University, Košice, Slovakia

Introduction

The final extent of brain damage after ischaemic insult results from a combination of processes that are initiated by the ischaemia itself and by a series of subsequent reactions to it in the case of circulation renewal. Because very early blood supply restoration is a crucial step for minimizing ischaemia impact, prolonged or permanent blockade of blood circulation in brain tissue represents a serious problem in clinical practice. At present, the phenomenon of ischaemic tolerance has become an attractive strategy for improving ischaemia outcome. There are several possibilities for how to boost post-ischaemic neuronal survival (especially post-conditioning), such as repeated short ischaemia, pharmacological treatment and remote limb tourniquet (Zhao et al. 2012). Based on experimental practice (and as noted below), the right timing of an intervention is essential for a good outcome (Durukan and Tatlisumak 2010).

In general, the affected brain tissue can be divided into two parts, the core and penumbra. The core represents the central part of the ischaemic region that is characterized by membrane depolarization and, in connection with this, a breakdown in energy metabolism. The energy metabolism in the surrounding tissue, the penumbra, is preserved; however, some metabolic, electrical and functional parameters of the tissue may be influenced (Astrup et al. 1981). Spread of the membrane depolarization to penumbra tissue during ongoing ischaemia results in expansion of the ischaemic core and therefore in expansion of the brain damage (Hartings et al. 2003; Ayata 2013). This process is not uniform in transient focal ischaemia models and depends strictly on secondary injury due to circulation renewal. On the other hand, in permanent models of brain ischaemia, this expansion is non-linear, spreading rapidly during the first 3 h but essentially terminated between the third and sixth hour of ischaemia (Hossmann 2008).

In ischaemia produced by MCAO, core neurons demonstrate the morphological and biochemical changes of necrotic cell death (Yao et al. 2001). In contrast to this, in the penumbra, ischaemia-induced events more often lead to programmed cell death (Lipton 1999) that seems similar to delayed neuronal death in ischaemia-sensitive neurons (selective vulnerable neurons) (Du et al. 1996; Endres et al. 1998). Post-ischaemic upstream death signals generated by cell membrane death receptors or by the release of death-inducing mitochondrial proteins activate downstream events that ultimately lead to DNA fragmentation and cell death. Released cytochrome C leads to procaspase-9 activation, which, in turn, cleaves and activates procaspase-3. Both caspase-9 and -3 activation has been implicated as a mechanism of neuronal cell death after ischaemia (reviewed in Plesnila et al. 2004). Moreover, the role of other factors, such as glutamate-mediated excitotoxicity, changes in the antioxidant activity of superoxide dismutase isoforms, and protein synthesis in ischaemia-affected tissue could be suitable markers of core spreading as well as for distinguishing the actual extent of the core/penumbra (Bonova et al. 2013).

As indicated above, the positive effect of therapeutic intervention in stroke models is primarily connected to the right timing of the intervention. In permanent ischaemia, the time window is limited by core spreading; thus, it is limited by the irreversible cellular breakdown of energy metabolism. The greatest potential should be expected while the penumbra has a maximum volume, i.e., within the first "golden" hour of blood restriction. During this time, the penumbra accounts for up to 50 % of the infarct volume (Saver et al. 2010). With ongoing ischaemia, the extent of the penumbra rapidly declines and after the third hour disappears almost completely (Hossmann 2012). From this point of view, it becomes very interesting to clarify the process of ischaemic damage spread from a reversible to an irreversible state. In the present paper, we monitored the clearest representatives of ischaemia-induced tissue damage and their evolution during the process of core expansion to its final state at three time points: (a) the first "golden" hour of ischaemia, (b) 3 hours and (c) the sixth hour of ischaemia when the process of core expansion has terminated.

Material and Methods

The experiments were carried out in accordance with the protocol for animal care approved by European Communities Council Directive (2010/63/EU). Every effort was made to minimize animal suffering and reduce the number of animals used. Adult male albino Wistar rats weighing 270–320 g were maintained on a 12-h light/dark cycle and given food and water ad libitum. Food was withdrawn 1 day before surgery.

Design of Experiment

Four groups containing five animals each were designed: the control group comprising sham control animals (also referred to as ischaemia 0 h) and three ischaemic groups with a different duration of ischaemia (1 h of ischaemia and 3 and 6 h of ischaemia). All animals were deeply anaesthetized with chloralhydrate at the appropriate experimental time and decapitated. The brain was removed and cut into 2-mm-thick slices by a rodent brain matrix RBM 4000C (ASI Instruments, USA) and processed for biochemical analysis with the exception of the third slice of brain tissue, which was designated for Evans Blue extravasation assay and immunohistochemical evaluation of NeuN positivity.

Middle Cerebral Artery Occlusion

Focal cerebral ischaemia was produced by right middle cerebral artery occlusion (MCAO) as described previously (Longa et al. 1989). The rats were anaesthetized with isoflurane (4 % initially, 1 to 1.5 % maintenance). Under an operating microscope, the right common carotid artery (CCA), the right external carotid artery (ECA) and the right internal carotid artery (ICA) were isolated, and a 6-0 silk suture was tied at the origin of the ECA and at the distal end of the ECA. A 4/0 nylon monofilament was introduced into the ECA and pushed up the ICA until light resistance was felt. The filament was inserted approximately 19 to 20 mm from the carotid bifurcation to effectively block the middle cerebral artery (MCA). The diameter of the tip of the suture was considered acceptable at around 300 μm. The suture remained inserted for 1, 3 or 6 h, after which the animals were decapitated. Control animals were subjected to the same surgical procedure without subsequent monofilament insertion (sham control=ischaemia 0 h). Local cerebral blood flow was measured to confirm the severity of MCA occlusion using a laser–Doppler flow meter (PeriFlux System 5000, Perimed AB, Sweden). A 407 probe with an adequate holder was situated on the skull over the MCA location (5 mm lateral and 1 mm posterior to the bregma). Only rats with blood flow reduced by more than 80 % were used for the experiments.

Neurological deficits were assessed in each animal on a numerical scale of 0–4 at 60 min of MCAO. The scoring system based on Bederson et al. (1986) was used: 0, no detectable deficits; 1, forelimb flexion and torso turning to the contralateral side when lifted by the tail; 2, same behaviour as grade 1 and decreased resistance to a lateral push; 3, same behaviour as grade 2 with unilateral circling; 4, no spontaneous walking and a depressed level of consciousness. Rats with a neurological deficit of less than 2 were excluded from the study.

Histological and Immunohistochemical Determination of Blood–Brain Barrier Disruption and Total Neuron Counts

One hour before decapitation of the animal and transcardial perfusion with ice-cold phosphate-buffered saline (PBS), Evans Blue dye (100 mg/kg) was injected into the right jugular vein. The third slice of brain tissue (corresponding to the dorso-lateral striatum) was used to assess blood–brain barrier (BBB) disruption based on extravasation of Evans Blue dye from the blood circulation into the brain tissue and for immunohistochemical determination of the neuronal count (NeuN positivity). Fixed and frozen brain tissue was sliced (thickness 30 μm) and assessed using a standard fluorescent microscope (Olympus, magnification×20).

For expression of BBB disruption, the mean fluorescence intensity of Evans Blue dye in pictures of the core and penumbra counted by Image J software was used (mean fluorescence intensity/image).

For immunohistochemistry, sections were incubated with mouse monoclonal anti-NeuN (1:400; Millipore) overnight at 4 °C and subsequently with fluorescent secondary Alexa 488 goat anti-mouse (1:200; Molecular Probes) antibodies for 2 h at room temperature and then cover slipped for image analysis. Microphotographs were taken from the ipsilateral and contralateral sides of the striatum (core and penumbra) with a×20 objective and NeuN-positive cells were counted. The localization of core and penumbra was established based on Hata et al. (2000). The core region was localized in the central part of infarcted tissue that is affected since very early ischaemia, the penumbra region close to the border of maximal infarct volume in order to minimize effect of core overlay up to 6 h of ischaemia.

Tissue Processing for Western Blot Analysis and Assessment of Glutamate Concentration

Regions corresponding to the core and penumbra from the right (ipsilateral) and left (contralateral) hemispheres designated for biochemical analysis were dissected according to Ashwal et al. (1998) with modification (Tsantes et al. 2013). The core (striatum and overlying cortex) was separated from the penumbra (adjacent cortex) by transverse diagonal cuts at approximately the '2 o'clock' and '5 o'clock' positions (ipsilateral hemisphere) and the '10 o'clock' and '7 o'clock' positions (contralateral hemisphere), respectively.

Sections of the tissue were weighed and homogenized in homogenization buffer (20 mM Tris–HCl, 50 mM magnesium acetate, 140 mM KCl, 1 mM EDTA, 2 mM EGTA and 1 mM DTT, pH 7.5 with added Protease Inhibitor Cocktail Tablets, Roche, Germany) and then centrifuged at 12,000*g* (15 min, 4 °C). Post-mitochondrial supernatants were aliquoted and frozen at −80 °C until analysis. Total protein concentrations in samples were determined using the method described by Bradford (1976) and BSA was used to establish a standard curve.

Concentration of Glutamate

Glutamate concentrations in the post-mitochondrial supernatants of core and penumbra tissue were measured by a modified enzymatic–fluorimetric method (Kravcukova et al. 2009) based on an assay described in Graham and Aprison (1966). First, aliquots of post-mitochondrial supernatant were thawed and precipitated using cold 1 M PCA at a ratio of 1:19 and centrifuged; the supernatant was then used for the glutamate assay. Glutamate concentrations in the samples were determined by fluorimetric detection of NADH resulting from the reaction of glutamate and NAD^+ catalyzed by glutamate dehydrogenase. The glutamate concentration is directly proportional to the concentration of NADH in a reaction. Briefly, 10 μl of supernatant was pipetted into a black 96-well plate, and 190 μl of reaction buffer (0.25 M hydrazine hydrate/0.3-M glycine buffer, pH 8.6) containing 200 nM NAD^+ and 15 U of glutamate dehydrogenase was added. After 30 min of incubation at RT, the fluorescence intensity of the final product (NADH) was read on a Synergy™ 2 Multi-Mode Microplate Reader (BioTek) at 460 nm with an excitation wavelength of 360 nm. The concentration of glutamate in tissue samples was normalized in accordance with the total protein concentration (μmol/mg of protein). All chemicals used for glutamate concentration measurements were purchased from Fluka.

Western Blot Analysis

Post-mitochondrial supernatants of equivalent protein content (50 μg) were resolved by SDS/PAGE (15 % gel for cytochrome C and 12 % gel for the rest) and electroblotted onto polyvinylidene difluoride (PVDF) membranes (Hybond-P PVDF membrane, GE Healthcare). After a 1-h blocking of non-specific binding sites with 5 % non-fat dry milk (5 %*w*/*v*) in PBS Tween-20 (0.1 %*v*/*v*), the membranes were incubated overnight (4 °C) with primary antibodies: mouse monoclonal anti-cytochrome C (1:1000, Abcam plc.), rabbit polyclonal anti-active caspase 3 (1:1000, Abcam plc.), rabbit monoclonal anti-caspase 9 (1:3000, Abcam plc.), goat polyclonal anti-beta actin (1:5000, Abcam plc.), rabbit Mn superoxide dismutase (SOD) (1:5000, Enzo Life Sciences) and rabbit Cu/Zn SOD (1:5000, Enzo Life Sciences). The membranes were washed in PBS Tween-20 (0.1 %*v*/*v*) and then incubated with secondary horseradish-peroxidase-conjugated antibody for 1 h at RT (1:10,000, goat anti-rabbit IgG (H&L) HRP conjugated; goat anti-mouse IgG (H&L) HRP conjugated; donkey anti-goat IgG (H&L) HRP conjugated, Agrisera). Bound antibody was revealed by means of enhanced chemiluminescence (SuperSignal® West Pico Chemiluminescent Substrate,

Thermo Scientific). The chemiluminescent signal was captured by a Fusion FX Chemiluminiscence system (Vilber Lourmat), and quantification of band intensities was performed with densitometric measurement software for image analysis (Bio-1D++, Vilber Lourmat). Results were expressed as relative density values calculated by dividing the per cent values in each row by the control sample's per cent value (beta actin).

Statistical Analysis

Data are calculated as the mean±SEM. Statistical analysis was performed with one-way ANOVA followed by the Dunnett post hoc test. $p<0.05$ was considered to be statistically significant.

Results

Integrity of the Blood–Brain Barrier

The Evans Blue extravasation method for post-ischaemic determination of BBB condition was used. The integrity of the BBB over the time course from 1 to 6 h of blood supply restriction was the most affected in the core of the ipsilateral hemisphere. We observed that fluorescence intensity in the core was increased by about 476±77 % in the first hour and up to 607±68 % 6 h after occlusion of the MCA. In the penumbra region of the same hemisphere, significantly elevated emission of Evans Blue dye was detected 1 (235.7±66 %), 3 (280.5±53 %) and 6 (269.5±46 %) hours after blood supply restriction (Fig. 1).

No significant rise in the fluorescence emission of EB dye was detected in the core and penumbra of the contralateral hemisphere (Fig. 1). The increasing intensity was more or less homogenous in both regions during the whole time window of ischaemia.

Neuron Counts

The number of NeuN-positive cells (neuron count) decreased after initiating ischaemia in the whole brain, particularly in the ischaemia core region (Fig. 2). The neuron count in the ischaemic core dropped gradually by about 81.9 % compared to control by the sixth hour (neuron count in the control 1335± 75 NeuN-positive cells/mm^2). A significant response to blood supply restriction was also clearly detected in the penumbra of the ipsilateral hemisphere after the first hour of occlusion.

The results of our experiments confirm that the ischaemic condition affected the total neuron count in the dorso-lateral striatum of the opposite, contralateral, hemisphere as well. Up to 3 h of MCA occlusion produced a slight loss of NeuN positivity (ranging from 1087.2±78.6 to 1173.8±80.5 NeuN-positive cells/mm^2). In contrast, a significant decrease in the quantity of neurons was seen after 6 h of brain ischaemia (ranging from 856.7±101 NeuN-positive cells/mm^2 in the core to 917.5±98 NeuN-positive cells/mm^2 in the penumbra).

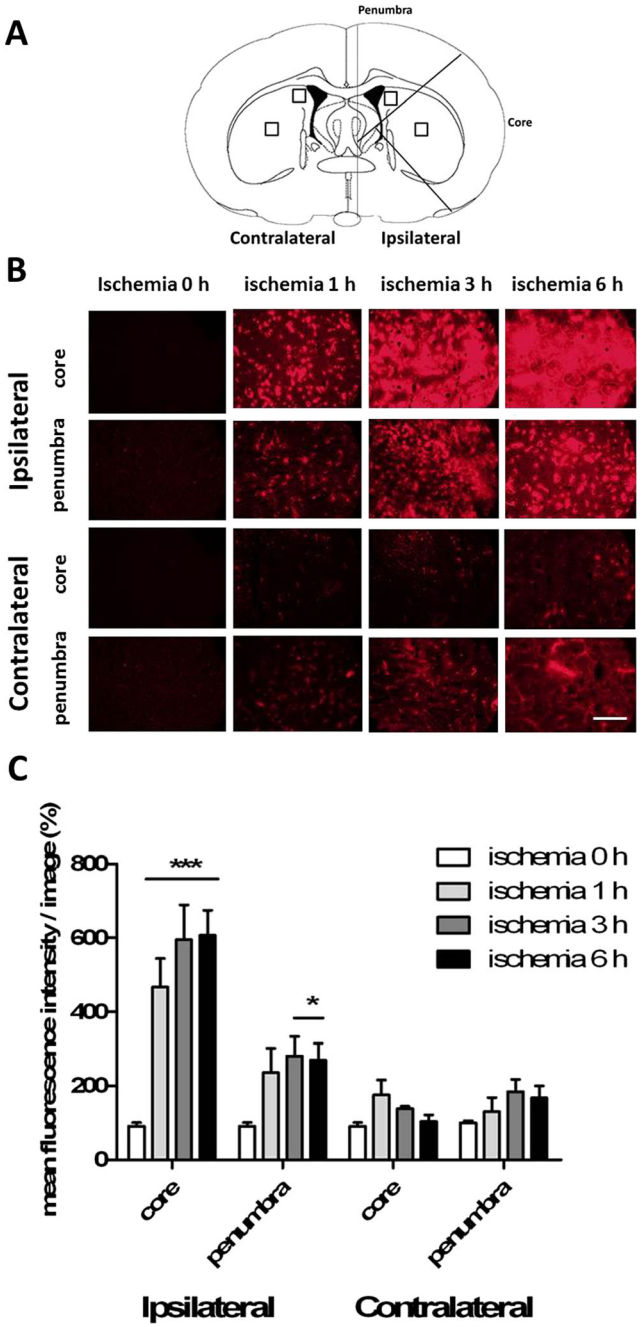

Fig. 1 Evans Blue dye extravasation. **a** Schematic drawing of brain areas used for monitoring of Evans Blue dye fluorescence intensity. *Squares on the drawing* show regions of photomicrograph images. **b** Representative microscopic pictures of core and penumbra tissue of ipsilateral and contralateral hemispheres after intravenous application of Evans Blue dye. *Bar*=200 μm. **c** Graphically processed results of Evans Blue extravasation in a control animal (ischaemia 0 h) and animals subjected to 1, 3 and 6 h of occlusion of the middle cerebral artery. *$p<0.05$, **$p<0.01$, ***$p<0.001$

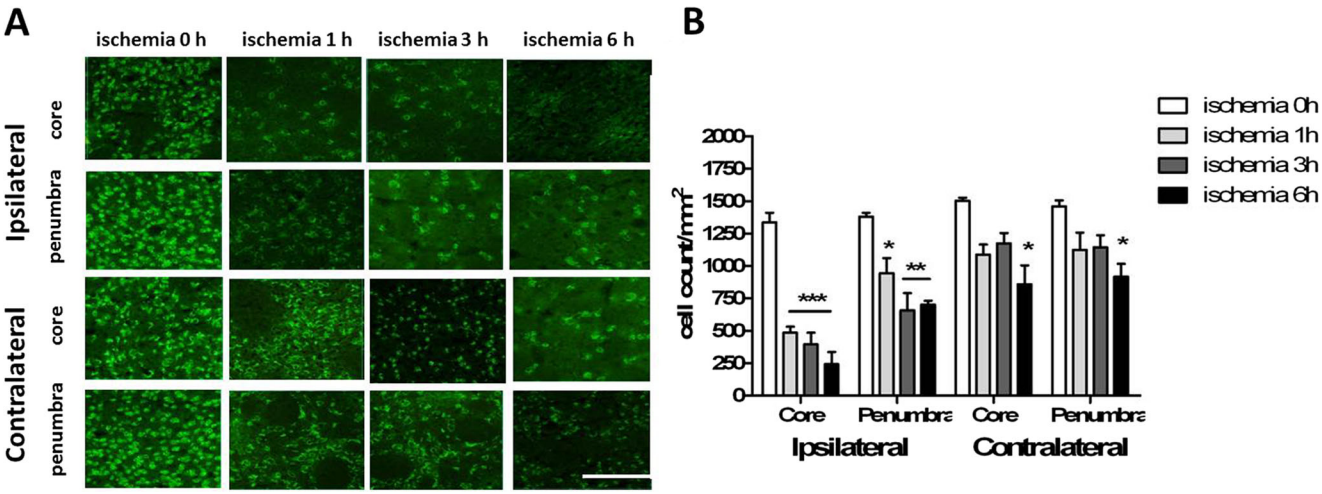

Fig. 2 Count of NeuN-positive cells in the core and penumbra regions of the ipsilateral and contralateral hemispheres. **a** Representative microscope images of NeuN-positive cells in core and penumbra regions of the ipsilateral and contralateral hemispheres. *Bar*=50 μm. **b** Graphically processed results of NeuN-positive cell evaluation in brain slices of a control animal (ischaemia 0 h) and animals subjected to 1, 3 and 6 h of occlusion of the middle cerebral artery. *$p<0.05$, **$p<0.01$, ***$p<0.001$

Post-ischaemic Tissue Glutamate Concentration

No significant changes in glutamate content were observed in post-mitochondrial supernatants from the core and penumbra regions of either hemisphere in the control group (ranging from 0.264±0.003 to 0.275±0.003 μmol/mg of protein); however, significant changes in glutamate level were found in the ipsilateral and contralateral hemispheres of the ischaemia groups (Fig. 3).

In the core of the injured brain site, glutamate concentration rose rapidly by about 46 % (0.508±0.026 μmol/mg of protein) after 1 h of ischaemia and remained at approximately the same level after 3 h (0.491±0.043 μmol/mg of protein). With the passage of more time, after 6 h of MCA occlusion, the glutamate content in the ischaemia core increased more than 2-fold compared to control (ischaemia 0 h) and reached 0.663 ±0.023 μmol/mg of protein, i.e. an elevation of about 141 %. In the penumbra of this hemisphere, glutamate levels increased within the first hour of ischaemia by about 42 % (0.428±0.02 μmol/mg of protein). After 3 h of ischaemia, the level of glutamic acid reached 0.462±0.04 μmol/mg of protein and peaked at the sixth hour of MCA occlusion (0.472±0.035 μmol/mg of protein).

Surprisingly, an impact of the ischaemic condition on the contralateral hemisphere was detected. We observed elevated levels of post-mitochondrial glutamate in the core as well as the penumbra throughout the entire studied period, most significantly after 6 h of MCA restriction (Fig. 3). In the core, the glutamate level rose by about 22.5 % (0.341±0.01 μmol/mg of protein) 1 h after ischaemia induction and stayed almost unchanged up to the third hour (0.335±0.032 μmol/mg of protein). Similar values were also detected in the penumbra region (0.342±0.005 μmol/mg of protein after the first hour of ischaemia; 0.381±0.05 μmol/mg of protein at the third hour of ischaemia). Six hours of MCA occlusion led to a significant elevation of glutamic acid in the core (0.414±0.003 μmol/mg of protein) as well as in the penumbra (0.381±0.021 μmol/mg of protein) of this hemisphere.

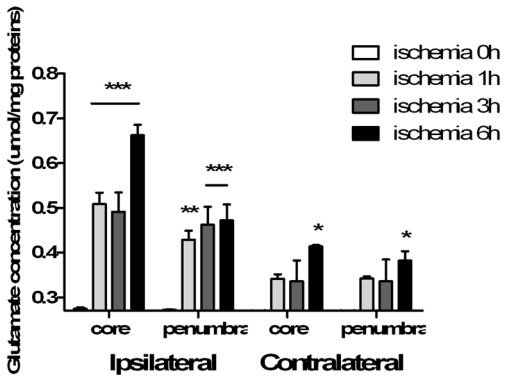

Fig. 3 Glutamate concentration in the core and penumbra regions of the ipsilateral and contralateral hemispheres after different periods of ischaemia. *$p<0.05$, **$p<0.01$, ***$p<0.001$

Western Blot Analysis

Enzyme Antioxidant Response of Brain Tissue to Ischaemia

Semiquantitative analysis of the CuZn SOD content in post-mitochondrial supernatants of the penumbra and core confirmed the tissue enzyme antioxidant response to the ischaemic condition in the ipsilateral hemisphere (Fig. 4). In the ischaemic core, the relative density of CuZn SOD decreased significantly from 0.725±0.065 in the control to 0.433±0.034 in the experimental group of animals that were exposed to 6 h of ischaemia. In the penumbra of the same hemisphere, the content of this enzyme rose by about 34.5 % during the first

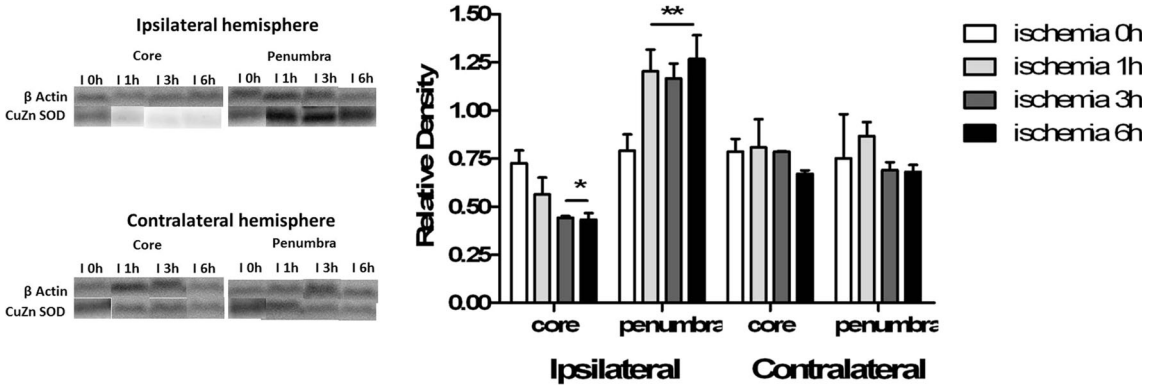

Fig. 4 Western blot determination of CuZn SOD content in the core and penumbra of the ipsilateral and contralateral hemispheres at four ischaemia time points. *$p<0.05$, **$p<0.01$, ***$p<0.001$

hour and stayed at approximately the same level up to the sixth hour of ischaemia (1.267±0.123).

In contrast to this, CuZn SOD density in the contralateral brain hemisphere differed only minimally compared to the control. We observed only slight insignificant reductions of CuZn SOD positivity in the core (by about 14.7 %) and penumbra (by about 10 %) after 6 h of reduced blood supply.

Mitochondrial Damage Evaluation

Over time, the blood restriction caused a release of mitochondrial Mn SOD enzyme from the mitochondria into the cell cytosol of affected brain tissue due to mitochondrial membrane disruption. While there was no significant elevation in the Mn SOD level in the whole brain (post-mitochondrial supernatant, respectively) during the first hour of blood supply restriction, in the ipsilateral hemisphere, its relative density was increased significantly since the third hour (Fig. 5). Mn SOD density in the ischaemic core rose more than 4.4-fold since the third (2.62±0.47) up to the sixth hour (2.53±0.29) of MCA occlusion. The level of this enzyme in the penumbra was even higher, its relative density reaching values of 4.23±0.79 3 h and 3.9±0.72 6 h after MCA occlusion. Insignificant changes in Mn SOD content (although elevated) were detected throughout the entire study period in the contralateral hemisphere.

Semiquantitative Evaluation of Enzymes Involved in the Process of Apoptosis

The first signals for apoptosis-linked enzymes in brain tissue were observed after 3 h of MCAO occlusion. All of the enzymes were detected in both the ischaemia-affected and the contralateral hemisphere as well (Fig. 6).

Cytochrome C The highest density of this mitochondrial enzyme in mitochondria-free cell cytosol was detected in the core region of the ischaemic hemisphere where it reached values of 0.76±0.033 and 1.02±0.092 after 3 and 6 h, respectively. In the rest of the brain (including the contralateral hemisphere), the level of cytochrome C was approximately equal (Fig. 6a) (i.e. after 3 h of MCA occlusion, the cytochrome C density ranged from 0.45±0.1 in the ischaemic penumbra to 0.68±0.02 in the contralateral penumbra, and after 6 h, it

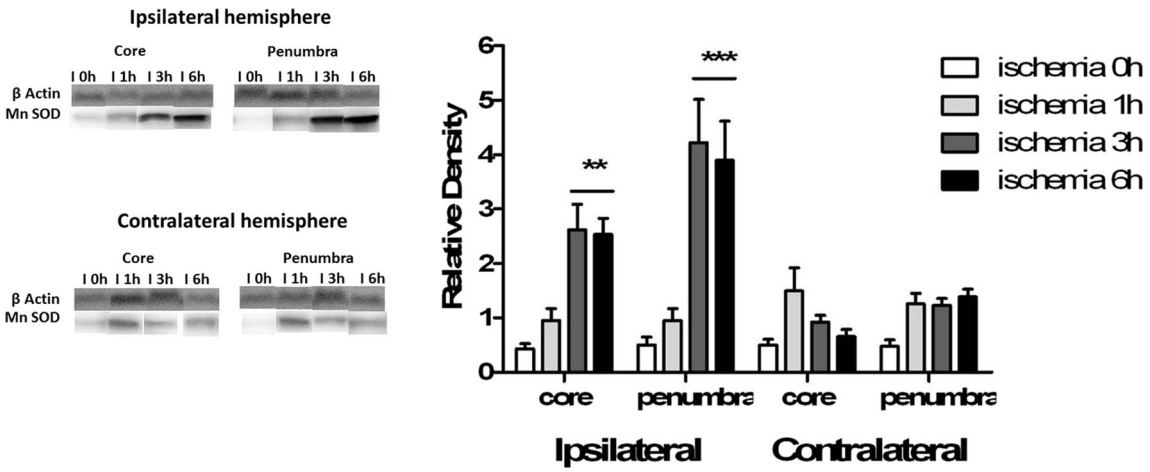

Fig. 5 Western blot determination of Mn SOD content in the core and penumbra of the ipsilateral and contralateral hemispheres at four ischaemia time points. *$p<0.05$, ***$p<0.001$

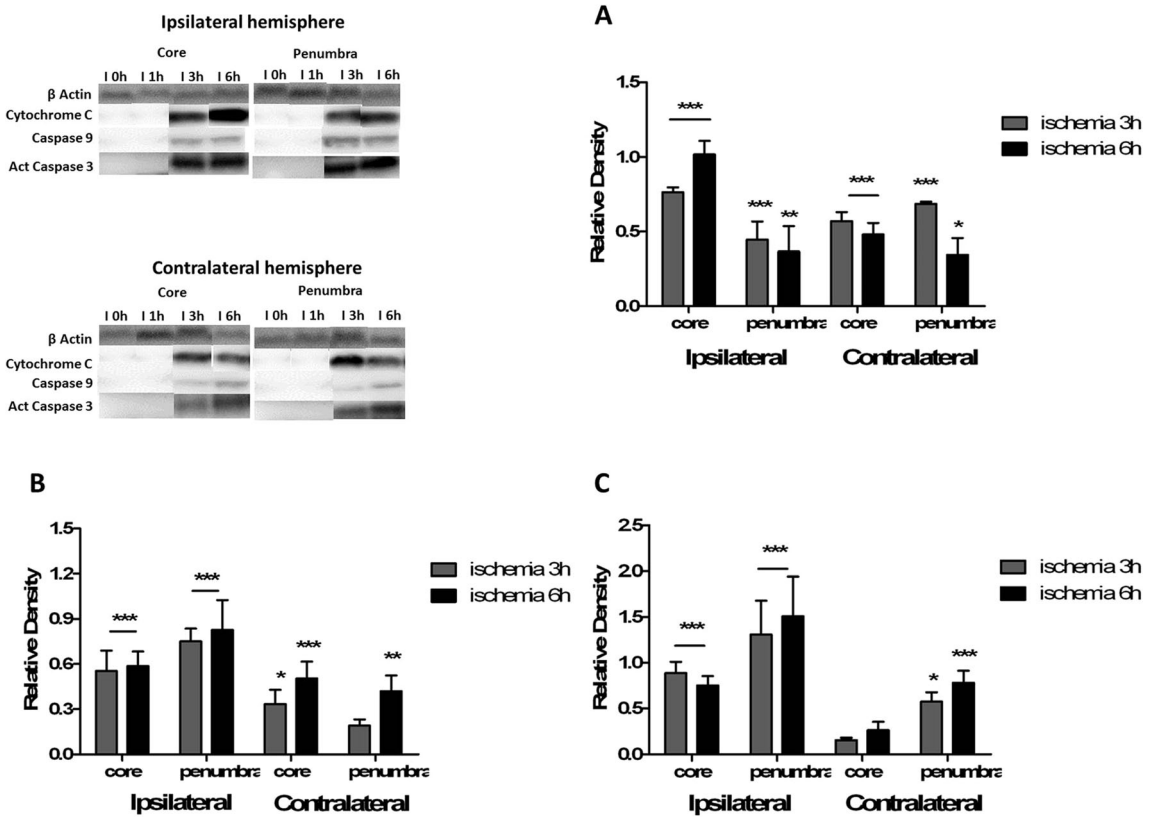

Fig. 6 Western blot determination of apoptosis-linked enzymes in the core and penumbra of the ipsilateral and contralateral hemispheres at four ischaemia time points. *$p<0.05$, **$p<0.01$, ***$p<0.001$. **a** Relative density of cytochrome C. **b** Relative density of caspase 9. **c** Relative density of active caspase 3

ranged from 0.365±0.17 in the ischaemic penumbra to 0.48± 0.076 in the contralateral core).

Caspase 9 As in the previous section, caspase 9 positivity was observed in the whole brain after both intervals of ischaemia (Fig. 6b). The highest level of this enzyme was detected in the ischaemic penumbra after 6 h of blood supply restriction (0.83 ±0.19). Relatively stable (but lower) caspase 9 levels were measured in the core of the ischaemia-affected hemisphere after both periods (0.55±0.14 after 3 h and 0.59±0.72 after 6 h).

In the contralateral hemisphere, the content of caspase 9 rose continuously. The maximum enzyme density was detected after 6 h of MCA occlusion in the core region (0.5±0.1).

Caspase 3 The density of this enzyme started to rise after 3 h of ischaemia (Fig. 6c). Caspase 3 positivity in the ischaemic core reached a value of 0.887±0.1. The highest level during this time interval was identified in the ischaemic penumbra (1.3±0.3). After 6 h of MCA occlusion, caspase 3 content was slightly decreased in the core (0.75±0.1) as well as in the penumbra of the ischaemic hemisphere (1.5±0.41). Moreover, elevated levels of caspase 3 were observed in the contralateral brain hemisphere since the third hour of ischaemia, beginning with a gentle increase in the core region followed by a significant increase in the penumbra.

Discussion

In the presented paper, we provide information about the pattern (scheme) of development of ischaemia-triggered agents during brain infarct evolution. We monitored these agents during three important time periods: (1) from the beginning of ischaemia to 1 h of blood supply restriction, i.e. the time with the largest extent of the penumbra and the greatest therapeutic potential, (2) 3 h of ischaemia, i.e. the time when the ischaemic core grows continuously into the penumbra region and (3) after 6 h of blood supply restriction, at which point the core has reached its maximum extent (Hossmann 2008).

Obviously, the general validity of the data is limited by the fixed localization of the core and penumbra during the dynamic process of infarct evolution (tissue section representing the core and penumbra, respectively). In the present paper, the core region was destined in the central part of infarcted tissue that is affected since very early ischaemia, the penumbra close to the border of maximal infarct volume. However, the penumbra region was designed in order to minimize the effect of core overlay; this could be taken into account with ongoing ischaemia, especially at ≥6 h of ischaemia when the penumbra has successively disappeared (Hata et al. 2000). On the other side, due to the infarct spreading, the core section has been ‘enriched’ from time period to time period.

One of the very first events after ischaemia initiation is disruption of the blood–brain barrier, which contributes to the cerebral infarction and the expansion of neuronal damage (Liu et al. 2012). The BBB represents a normal and highly effective way to protect sensitive brain tissue against different harmful agents. After ischaemia, its integrity is affected, resulting in penetration of inflammatory cells, high-molecular-weight molecules and fluid into the brain, causing oedema and cell death (Fishman 1975). The simplest method of studying BBB permeability is to measure tracer penetration into the brain after peripheral injection. Evans Blue dye (961 Da) is perhaps the most widely used in experimental animals because of its ability to bind to serum albumin (69, 000 Da), thus representing a high-molecular-weight protein tracer in the circulation (Saria and Lundberg 1983). Our results showed that the integrity of the BBB in the ischaemia-affected hemisphere was strongly impaired after the first hour of blood supply disruption and then remained in approximately the same condition with further passage of time. Moreover, the neuron count in this region significantly decreased, especially in the infarct area. Taking into account the concept of the 'golden' hour described above (in the context of improving post-ischaemic neuronal survival), we suggest that the maintenance of blood–brain barrier integrity does not play a crucial role in limiting the final infarct size, although its associated role in the development and progress of ischaemia-induced brain tissue damage cannot be questioned.

Another associated aspect of ischaemic brain tissue damage is glutamate-mediated excitotoxicity. Increased release of glutamate into the extracellular spaces around neurons caused by membrane depolarization leads to glutamate-mediated neurotoxicity due to overproduction of ROS and elevation of oxidative stress (Arundine and Tymianski 2004; Abou-Sleiman et al. 2006). During permanent blockade of the MCA, we observed increases in glutamate in the ischaemic hemisphere after the first hour of occlusion. The highest level of this excitotoxic agent was detected in the core region due to the processes triggered by direct blood supply restriction, while lower glutamate release was detected in penumbra tissue, partially supported via collaterals and the contralateral hemisphere. Longer times of ischaemia led to a progressive elevation of glutamate content, both directly in the ischaemic core as well as in the rest of the brain, suggesting its role in infarct expansion.

Elevated tissue glutamate content (as well as other agents monitored in this study) in the peri-infarct area could be explained by the spread of cellular depolarization from the site of origin through electrochemically neural tissue, i.e. by the spreading depression. Spreading depression may be triggered by high $[K^+]_0$ and glutamate levels in the ischaemic core and actively propagate tissue depolarization, ionic imbalances, and glutamate release into adjacent tissue. In the injury penumbra, where blood supply is compromised, spreading depression waves cause further reductions in tissue PO_2 and exacerbate metabolic stress–failure (Somjen 2001). In this context, these waves are referred to as peri-infarct depolarizations (PIDs), reflecting their pathogenic role and similarity to anoxic depolarization. In focal cerebral ischaemia, PIDs cause an expansion of core-infarcted tissue into adjacent penumbral regions of reversible injury and have been shown to occur through 6 h after injury. In permanent MCAO, PIDs occurred in a biphasic pattern with a mean of 78 events over 2–24 h. Parameters of secondary phase PID incidence correlated with infarct volumes in transient and permanent ischaemia models (Hartings et al. 2003).

SOD activity plays an indispensable role in the detoxification of superoxide radicals overproduced during and after an ischaemic event and also plays an important role in the defence against ischaemic brain damage (Li et al. 1998; Kawase et al. 1999; Danielisova et al. 2005). Measurement of the cytoplasmic form of SOD in the ischaemic core showed a gradual decline in density up to 6 h of MCA occlusion that could be explained by protein synthesis blockade induced by energy failure. In contrast to this, an elevated density of this enzyme was detected in the penumbra region. This suggests a greater requirement in the penumbra tissue for this antioxidant enzyme, which is ensured by collateral support of sufficient energy metabolism.

Three main components in the apoptotic machinery have been highlighted in the present paper: cytochrome C, caspase 9 and caspase 3. Cytochrome C is released from the mitochondria into the cytosol of the cell, activating a cascade reaction that leads to apoptotic cell death. During our study of infarct evolution in the permanent model of MCAO, we were unable to detect cytochrome C in post-mitochondrial supernatants after the first hour of occlusion. This observation reflects continuing integrity of mitochondrial membrane up to the first hour of ischaemia that was subsequently disrupted. From the third hour of ischaemia, its density rose significantly onwards in whole brain, especially in the ischaemic core. A downstream enzyme in the apoptotic cascade, caspase 9, was detectable from the third hour as well, reflecting its elevated production and/or increased release from mitochondria. In neuronal cell culture models as well as in animal models of transient global cerebral ischaemia, caspase 9 release from mitochondria and accumulation in nuclei were observed in hippocampal and other vulnerable neurons exhibiting early post-ischaemic changes preceding apoptosis (Krajewski et al. 1999). In response to caspase 9, a similar pattern could be seen in the tissue level of active caspase 3. Caspase 3, the effector of the apoptotic signalling pathway, is expressed, activated, and cleaved in cerebral ischaemia. The active form of caspase 3 is elevated in the process of apoptotic cell death (Namura et al. 1998). In our experiment, we clearly confirmed that the active form of caspase 3 was undetectable during the first hour of ischaemia in whole brain. Starting in the third

hour of MCA occlusion, activation of this enzyme commenced in the ischaemia-damaged hemisphere and then was more or less unchanged up to 6 h. The highest level of active enzyme could be detected in the ischaemic penumbra, i.e. expansion of the ischaemic core into the penumbra caused by prolonged occlusion time could be expected.

One of the events reflecting serious cell damage in brain tissue caused by prolonged ischaemia is mitochondrial damage. In this experiment, the presence of the mitochondrial isoform of SOD in the cell cytosol was studied as a marker of mitochondrial membrane disruption. Based on our results, we can state that ischaemia did not affect mitochondria membrane integrity up to 1 h of blood supply restriction. Similar to the apoptosis-associated enzymes described above, significantly increased release of Mn SOD from mitochondria into the cell cytoplasm was detected since the third hour of ischaemia. These results may be connected to a progressive reduction in the number of dorso-lateral striatum neurons. Interestingly, the highest level of Mn SOD was cumulated in the penumbra region. This observation may suggest progressive mitochondrial damage in ischaemia-affected brain tissue, but, taking into account mitochondria as a possible source of certain cytosolic enzymes, it would explain the rapid elevation in concentration of cytochrome C and caspase 9 in the cell cytosol as well. Noshita et al. (2001) suggested that Mn SOD might affect cytochrome C translocation and downstream caspase activation in the mitochondrial-dependent cell death pathway after transient focal brain ischaemia in a mouse model. Two hours after reperfusion, cytochrome C and caspase 9 were observed in the cytosol and were significantly increased in Mn SOD-deficient mutants compared with wild-type mice. Therefore, we expect that this mechanism could contribute to accelerating apoptotic processes during ongoing ischaemia (beyond the first hour of ischaemia) and thus in the rapid non-linear expansion of the ischaemic core.

Additionally, our results clearly confirm that the final effect of MCA blockade of one hemisphere produces a whole brain response. Given that there are some literature reports connecting transient focal ischaemia to contralateral changes (listed below), we provide evidence about similar dramatic changes in a model of permanent focal ischaemia. Redecker et al. (2002) reported the occurrence of various functional alterations within structurally intact brain regions ipsilateral and contralateral to the focal ischaemia. These changes were termed remote effects. Remote contralateral effects were attributed to the extensive interhemispheric connections that exist in the rat cortex.

In the present paper, we provide evidence about the decreased total number of neurons in the whole contralateral hemisphere after the first hour of ischaemia, with maximal elimination of NeuN-positive cells 6 h after the attack. Despite this, we were unable to detect degenerating neurons (FloroJade B staining) at this time point even in the ipsilateral site (data not included). The integrity of the BBB was slightly disrupted and allowed penetration of high-molecular-weight complexes of Evans Blue dye–serum albumin into brain tissue. Glutamate content rose as well, especially late in ischaemia. In contrast to this, the density of the antioxidant enzyme CuZn SOD decreased only slightly in this hemisphere.

The pathological changes in remote brain areas likely indicate chronic ischaemic diaschisis, which should be considered in developing treatment strategies for stroke (Garbuzova-Davis et al. 2014). The authors have observed significant extravasation of Evans Blue dye 30 days after transient MCAO and registered several ultrastructural changes in the motor cortex and striatum of this hemisphere, including vacuolated endothelial cells with large autophagosomes, degenerated pericytes displaying mitochondria with cristae disruption, degenerated astrocytes and perivascular oedema and the appearance of parenchymal astrogliosis. The authors suggest that this vascular damage in remote brain areas opposite to the initial stroke insult might indicate ongoing pathological vascular changes in association with chronic diaschisis. As could be expected from the results described above, Dief and co-workers (2008) observed apoptotic TUNEL-positive cells 7 days after transient MCAO. Although we did not study the direct appearance of apoptotic cells in the contralateral site, our work provides evidence about markers linked to apoptosis. After the third hour of permanent blockade of the blood supply to the right MCA, there were elevated levels of cytoplasmic cytochrome C, caspase 9 and the active form of caspase 3 in the core as well as in the penumbra of the contralateral (left) hemisphere.

In conclusion, we can summarize that the basis for the ‘golden hour’ phenomenon could be the preserved integrity of mitochondrial membrane and the incompletely developed process of apoptosis. During the first hour of ischaemia, we did not detect the appearance of certain enzymes typical of the apoptotic pathway; however, the direct expression of other ischaemia-linked changes (disrupted BBB and increased glutamate level) was also detectable in this early period of MCA occlusion. The apoptotic pathway was clearly developed after 3 h of ischaemia when the mitochondrial enzyme release in cell cytoplasm was detected. We suppose that the activated apoptotic pathway could be connected to the relatively low potential of therapeutic intervention after this point. Moreover, the present results indicate the remote effect of an ischaemic insult manifested in direct morphological changes in BBB integrity as well as changes in intracellular signalling connected to apoptosis after prolonged brain ischaemia.

Acknowledgments This study was supported by the Slovak Grant Agencies VEGA 2/0012/15 and VEGA 2/0045/15.

Conflict of interest The authors have no conflicts of interest related to this work.

References

Abou-Sleiman PM, Muqit MM, Wood NW (2006) Expanding insights of mitochondrial dysfunction in Parkinson's disease. Nat Rev Neurosci 7:207–219

Arundine M, Tymianski M (2004) Molecular mechanisms of glutamate-dependent neurodegeneration in ischemia and traumatic brain injury. Cell Mol Life Sci 61:657–668

Ashwal S, Tone B, Tian HR, Cole DJ, Pearce WJ (1998) Core and penumbral nitric oxide synthase activity during cerebral ischemia and reperfusion. Stroke 29:1037–1046, **discussion 1047**

Astrup J, Siesjo BK, Symon L (1981) Thresholds in cerebral ischemia - the ischemic penumbra. Stroke 12:723–725

Ayata C (2013) Spreading depression and neurovascular coupling. Stroke 44:S87–S89

Bederson JB, Pitts LH, Tsuji M, Nishimura MC, Davis RL, Bartkowski H (1986) Rat middle cerebral artery occlusion: evaluation of the model and development of a neurologic examination. Stroke 17:472–476

Bonova P, Burda J, Danielisova V, Nemethova M, Gottlieb M (2013) Development of a pattern in biochemical parameters in the core and penumbra during infarct evolution after transient MCAO in rats. Neurochem Int 62:8–14

Bradford MM (1976) A rapid and sensitive method for the quantitation of microgram quantities of protein utilizing the principle of protein-dye binding. Anal Biochem 72:248–254

Danielisova V, Nemethova M, Gottlieb M, Burda J (2005) Changes of endogenous antioxidant enzymes during ischemic tolerance acquisition. Neurochem Res 30:559–565

Dief AE, Jirikowski GF, El-Sabah Ragab K, Ibrahim HS (2008) Ipsilateral and contralateral cortical apoptosis in rats after unilateral middle cerebral artery occlusion. Anatomy 2:39–48

Du C, Hu R, Csernansky CA, Hsu CY, Choi DW (1996) Very delayed infarction after mild focal cerebral ischemia: a role for apoptosis? J Cereb Blood Flow Metab 16:195–201

Durukan A, Tatlisumak T (2010) Preconditioning-induced ischemic tolerance: a window into endogenous gearing for cerebroprotection. Exp Transl Stroke Med 2:2

Endres M, Namura S, Shimizu-Sasamata M, Waeber C, Zhang L, Gomez-Isla T, Hyman BT, Moskowitz MA (1998) Attenuation of delayed neuronal death after mild focal ischemia in mice by inhibition of the caspase family. J Cereb Blood Flow Metab 18:238–247

Fishman RA (1975) Brain edema. N Engl J Med 293:706–711

Garbuzova-Davis S, Haller E, Williams SN et al (2014) Compromised blood-brain barrier competence in remote brain areas in ischemic stroke rats at the chronic stage. J Comp Neurol 522:3120–3137

Graham LT Jr, Aprison MH (1966) Fluorometric determination of aspartate, glutamate, and gamma-aminobutyrate in nerve tissue using enzymic methods. Anal Biochem 15:487–497

Hartings JA, Rolli ML, Lu XC, Tortella FC (2003) Delayed secondary phase of peri-infarct depolarizations after focal cerebral ischemia: relation to infarct growth and neuroprotection. J Neurosci 23: 11602–11610

Hata R, Maeda K, Hermann D, Mies G, Hossmann KA (2000) Dynamics of regional brain metabolism and gene expression after middle cerebral artery occlusion in mice. J Cereb Blood Flow Metab 20:306–315

Hossmann KA (2008) Cerebral ischemia: models, methods and outcomes. Neuropharmacology 55:257–270

Hossmann KA (2012) The two pathophysiologies of focal brain ischemia: implications for translational stroke research. J Cereb Blood Flow Metab 32:1310–1316

Kawase M, Murakami K, Fujimura M, Morita-Fujimura Y, Gasche Y, Kondo T, Scott RW, Chan PH (1999) Exacerbation of delayed cell injury after transient global ischemia in mutant mice with CuZn superoxide dismutase deficiency. Stroke 30:1962–1968

Krajewski S, Krajewska M, Ellerby LM et al (1999) Release of caspase-9 from mitochondria during neuronal apoptosis and cerebral ischemia. Proc Natl Acad Sci U S A 96:5752–5757

Kravcukova P, Danielisova V, Nemethova M, Burda J, Gottlieb M (2009) Transient Forebrain ischemia impact on lymphocyte DNA damage, glutamic acid level, and SOD activity in blood. Cell Mol Neurobiol 29:887–894

Li Y, Copin JC, Reola LF, Calagui B, Gobbel GT, Chen SF, Sato S, Epstein CJ, Chan PH (1998) Reduced mitochondrial manganese-superoxide dismutase activity exacerbates glutamate toxicity in cultured mouse cortical neurons. Brain Res 814:164–170

Lipton P (1999) Ischemic cell death in brain neurons. Physiol Rev 79: 1431–1568

Liu R, Yuan H, Yuan F, Yang SH (2012) Neuroprotection targeting ischemic penumbra and beyond for the treatment of ischemic stroke. Neurol Res 34:331–337

Longa EZ, Weinstein PR, Carlson S, Cummins R (1989) Reversible middle cerebral artery occlusion without craniectomy in rats. Stroke 20:84–91

Namura S, Zhu J, Fink K, Endres M, Srinivasan A, Tomaselli KJ, Yuan J, Moskowitz MA (1998) Activation and cleavage of caspase-3 in apoptosis induced by experimental cerebral ischemia. J Neurosci 18:3659–3668

Noshita N, Sugawara T, Fujimura M, Morita-Fujimura Y, Chan PH (2001) Manganese superoxide dismutase affects cytochrome c release and caspase-9 activation after transient focal cerebral ischemia in mice. J Cereb Blood Flow Metab 21:557–567

Plesnila N, Zhu C, Culmsee C, Groger M, Moskowitz MA, Blomgren K (2004) Nuclear translocation of apoptosis-inducing factor after focal cerebral ischemia. J Cereb Blood Flow Metab 24:458–466

Redecker C, Wang W, Fritschy JM, Witte OW (2002) Widespread and long-lasting alterations in GABA(A)-receptor subtypes after focal cortical infarcts in rats: mediation by NMDA-dependent processes. J Cereb Blood Flow Metab 22:1463–1475

Saria A, Lundberg JM (1983) Evans blue fluorescence: quantitative and morphological evaluation of vascular permeability in animal tissues. J Neurosci Methods 8:41–49

Saver JL, Smith EE, Fonarow GC, Reeves MJ, Zhao X, Olson DM, Schwamm LH (2010) The "golden hour" and acute brain ischemia: presenting features and lytic therapy in >30,000 patients arriving within 60 minutes of stroke onset. Stroke 41:1431–1439

Somjen GG (2001) Mechanisms of spreading depression and hypoxic spreading depression-like depolarization. Physiol Rev 81:1065–1096

Tsantes A, Tsangaris I, Kopterides P et al (2013) The role of procalcitonin and IL-6 in discriminating between septic and non-septic causes of ALI/ARDS: a prospective observational study. Clin Chem Lab Med:1–8

Yao H, Takasawa R, Fukuda K, Shiokawa D, Sadanaga-Akiyoshi F, Ibayashi S, Tanuma S, Uchimura H (2001) DNA fragmentation in ischemic core and penumbra in focal cerebral ischemia in rats. Brain Res Mol Brain Res 91:112–118

Zhao H, Ren C, Chen X, Shen J (2012) From rapid to delayed and remote postconditioning: the evolving concept of ischemic postconditioning in brain ischemia. Curr Drug Targets 13:173–187